Evaluation of Solvent Accessibility to the [Fe_4S_4] Binding Pocket in Native and Tyr19 Mutant High Potential Iron Proteins by $^1H-^{15}N$ HMQC and ^{19}F NMR Experiments†

Dawei Li, Anshu Agarwal, and J. A. Cowan*,‡

Evans Laboratory of Chemistry, The Ohio State University, 100 West 18th Avenue, Columbus, Ohio 43210

Received September 1, 1995⊗

The solvent accessibility of *Chromatium vinosum* high potential iron protein (HiPIP) has been investigated by use of $^1H-^{15}N$ HMQC, and ^{19}F NMR spectroscopy. These NMR experiments indicate that solvent accessibility to the cluster core is similar, and minimal, for the reduced and oxidized states of native HiPIP, but increases significantly for mutant proteins (Tyr19Leu and Tyr19His). These results support a proposed role [Agarwal, A.; Li, D.; Cowan, J. A. *Proc. Natl. Acad. Sci. U.S.A.* **1995**, *92*, 9440−9444] for Tyr19 in maintaining hydrolytic stability of the [Fe_4S_4] cluster, and demonstrate a general strategy for mapping out the solvent accessibility of protein-bound metalloredox prosthetic centers.

Introduction

High-potential iron proteins (HiPIP's) represent one class of iron−sulfur cluster protein that has received extensive examination by spectroscopic and structural methods.[1−10] In spite of the increasing understanding of the electronic properties and functional chemistry of iron−sulfur proteins,[9−17] the functional roles of specific residues that form the cluster binding pocket are ill-defined. The [Fe_4S_4] center in *Chromatium vinosum* HiPIP is enclosed by several hydrophobic aromatic side chains from the C-terminal domain (residues 43 - 80) and a short portion of the N-terminal domain (residues 17−20).[8] This N-terminal sequence adopts an α-helical conformation and accommodates a conserved tyrosine residue that lies in close proximity to the reduced cluster.[14] Previously we have used ^{19}F NMR and site-directed mutagenesis to probe the chemistry of this site.[18,19] These studies provided information on the dynamics and bonding interactions of this residue with the cluster, and suggested a novel functional role for this residue. Kinetic studies of cluster stability, and two-dimensional COSY NMR data support a model where Tyr19 serves to maintain a hydrophobic barrier for exclusion of water from the cluster cavity.[19] Tyr19 mutant proteins demonstrated, to varying extents, the ability of water molecules to exchange with ionizable protons in the cluster binding pocket. Solvent accessibility results in facile oxidation of the cluster by atmospheric oxygen, with subsequent rapid hydrolysis of the [Fe_4S_4]$^{3+}$ core. A decrease in cluster stability in the presence of a polar solvent is consistent with previous studies of model complexes that demonstrate sensitivity of the oxidized [Fe_4S_4]$^{3+}$ core to solvolytic decomposition.[7,20,21]

The number and orientations of hydrophobic residues that surround the cluster, the extent of solvent accessibility, and the influence of the protein-derived electrostatic field have been cited as critical factors in the control of cluster reduction potentials ($E°$'s).[4,5] These issues are of general relevance for understanding the mechanisms employed by proteins for modulating the chemistry of protein-bound redox cofactors.[3−5] In this paper we evaluate the solvent accessibility of native and mutant HiPIP's by multinuclear NMR methods: in particular, by use of the $^1H/^2H$ exchange rates of backbone amide protons, evaluated by $^1H-^{15}N$ HMQC experiments, and from the isotopic perturbation of ^{19}F chemical shifts of fluorine-labeled native and mutant HiPIP's. The implications of these results for the understanding of the chemistry and physicochemical properties of protein-bound clusters and the functional role of hydrophobic residues in cluster binding pockets are discussed.

† Abbreviations: HiPIP, high potential iron protein; NMR, nuclear magnetic resonance; COSY, 2D correlation spectroscopy; HMQC, heteronuclear multiple quantum correlated spectroscopy.

‡ JAC is a Fellow of the Alfred P. Sloan Foundation, a Camille Dreyfus Teacher- Scholar, and a National Science Foundation Young Investigator.

⊗ Abstract published in *Advance ACS Abstracts,* February 1, 1996.

(1) Carter, C. W. Jr.; Kraut, J.; Freer; S. T.; Xuong, N. H.; Alden, R. A.; Bartsch, R. G. *J. Biol. Chem.* **1974**, *249*, 4212.
(2) Carter, C. W., Jr. In *Iron−Sulfur Proteins III* (Lovemberg, W. Ed.) pp. 157−204: Academic Press; NY, 1977.
(3) Rayment, I.; Wesenberg, W.; Meyer, T. E.; Cusanovich, M. A.; Holden, H. M. *J. Mol. Biol.* **1992**, *228*, 672−686.
(4) Langen, R.; Jensen, G. M.; Jacob, U.; Stephens, P. J.; Warshel, A. *J. Biol. Chem.* **1992**, *267*, 25625.
(5) Jensen, G. M.; Warshel, A.; Stephens, P. J. *Biochemistry* **1994**, *33*, 10911.
(6) Gaillard, J.; Albrand, J.-P.; Moulis, J.-M.; Wemmer, D. E. *Biochemistry* **1992**, *31*, 5632.
(7) Bruice, T. C.; Maskiewicz, R.; Job, R. C. *Proc. Natl. Acad. Sci. U.S.A.* **1975**, *72*, 231.
(8) Carter, C. W.; Kraut, J.; Freer, S. T.; Xuong, N. H.; Alden, R. A. *J. Biol. Chem.* **1974**, *249*, 6339.
(9) Bertini, I.; Capozzi, F.; Ciurli, S.; Luchinat, C.; Messori, L.; Piccioli, M. *J. Am. Chem. Soc.* **1992**, *114*, 3332.
(10) Bertini, I.; Gaudemer, A.; Luchinat, C.; Picioli, M. *Biochemistry* **1993**, *32*, 12887.
(11) Banci, L.; Bertini, I.; Dikiy, A.; Kastrau, D. H. W.; Luchinat, C. Sompornpisut, P. *Biochemistry* **1995**, *34*, 206.
(12) Bertini, I.; Brigaanti, F.; Luchinat, C.; Scozzafaia, A.; Sola, M. *J. Am. Chem. Soc.* **1991**, *113*, 1237.
(13) Mizrahi, I. A.; Meyer, T. E.; Cusanovich, M. A. *Biochemistry* **1980**, *19*, 4727.
(14) Przysieck, C. T.; Meyer, T. E. Cusanovich, M. A. *Biochemistry* **1985**, *24*, 2524.
(15) Cunningham, R. P. Asahara, H.; Bank, J. F.; Scholes, C. P.; Salerno, J. C.; Surerus, K.; Munck, E.; McCracken, J.; Peisach, J.; Emptage, M. H. *Biochemistry* **1989**, *28*, 4450.
(16) Emptage, M. H.; Kent, T. A.; Kennedy, M. C.; Beinert, H.; Munck, E. *Proc. Nat. Acad. Sci. U.S.A.* **1988**, *85*, 4674.
(17) Martin, A. E.; Burgess, B. K.; Stout, C. D.; Cash, V. L.; Dean, D. R. Jensen, G. M.; Stephenson, P. J. *Proc. Natl. Acad. Sci U.S.A.* **1990**, *87*, 598.
(18) Lui, S-M. and Cowan, J. A. *J. Am. Chem. Soc*. **1994**, *116*, 4483.
(19) Agarwal, A.; Li, D.; Cowan, J. A. *Proc. Natl. Acad. Sci. U.S.A.* **1995**,*92*, 9440−9444.
(20) Maskiewicz, R.; Bruice, T. C. *Proc. Natl. Acad. Sci. U.S.A.* **1977**, *74*, 5231.
(21) Maskiewicz, R.; Bruice, T. C. *Biochemistry* **1977**, *13*, 3024.

0020-1669/96/1335-1121$12.00/0

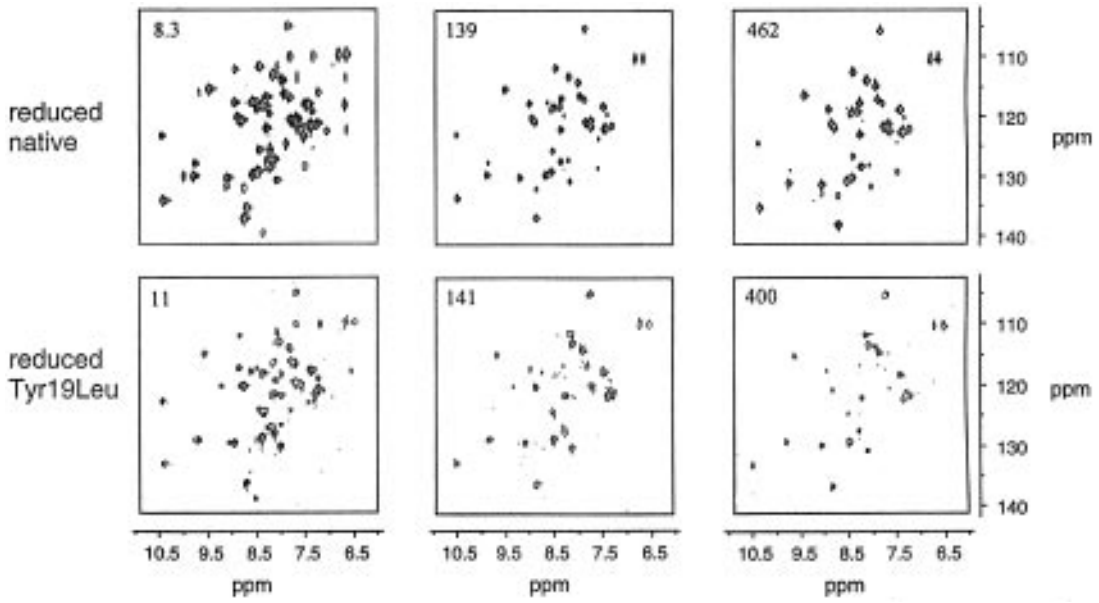

Figure 1. Examples of 2D $^1H-^{15}N$ HMQC spectra recorded for reduced recombinant native HiPIP and Tyr19Leu mutant HiPIP. For each group of spectra, the accumulated solvent exchange time at the end of each acquisition is indicated (in min) in the top left corner.

Experimental Methods

The preparation and purification of Tyr19 mutants has been described previously.[19,22] The preparation of uniformly ^{15}N-labeled and selectively ^{19}F-labeled HiPIP have also been described elsewhere.[23,24] NMR samples were prepared by dissolving a lyophilized sample of the protein, previously equilibrated in an appropriate buffer, in the solvent system of choice. The resulting sample solutions contained 10 mM sodium phosphate (pH 6.0) and 0.1 M NaCl. For the $^1H/^2H$ exchange experiments, the ^{15}N-labeled native and mutant HiPIP samples were lyophilized and then re-dissolved in D_2O immediately before NMR data acquisition. For the ^{19}F T_1 and isotope-effect measurements, the experiments were performed in both H_2O and D_2O buffered solvent.

The $^1H/^2H$ exchange experiments were performed on a Bruker DMX 600 instrument using a standard $^1H-^{15}N$ HMQC pulse sequence.[25,26] Taking advantage of the large memory and digital filter capabilities of the DMX instrument, the time typically spent on collecting dummy scans before t_1 data collection, and on saving each t_1 data set was eliminated, resulting in a considerable time saving. Each 2D HMQC data set was collected in a time-frame of less than 12 min for a spectrum defined by a 2K (t_2) $\times$ 256 (t_1) data matrix, with four scans for each t_1 increment and 16 dummy scans for the whole experiment (reduced from 4 $\times$ 256 dummy scans previously required on our AM 500 instrument). The delay time that distinguished each experiment was calculated from the time when the lyophilized sample was dissolved in D_2O, to the endpoint of each experiment. Cross-peak intensities were found to diminish with increasing delay time.

^{19}F NMR spectra were acquired on a Bruker AM 250 spectrometer at 235.36 MHz. Experimental details for measurement of ^{19}F T_1 relaxation times and isotope effects have been described elsewhere.[24] In these experiments, all ^{19}F NMR spectra were recorded with ^1H broad-band decoupling through the entire experiment to eliminate the possibility of contributions from cross-relaxation to the observed T_1 relaxation time. All experiments were performed at 303 K with 16 K data points of memory. The ^1H spectra were referenced to TMS and ^{19}F spectra were referenced to TFA.

Results

Previous studies of Tyr19X mutants of *C. vinosum* HiPIP have demonstrated decreasing cluster stability in the following order: X = Phe > Trp > Leu > His > Arg > Cys > Gln > Ser.[19] These studies show that when Tyr19 is replaced by either small (Leu) or polar (His, Arg, Cys, Gln, or Ser) residues the cluster becomes less stable. This arises from facile oxidation of the solvent-exposed cluster, which in turn results in significant hydrolytic instability. Solvent accessibility to the hydrophobic cluster-binding pocket appears to be sensitive to the size and polarity of the residue at position 19. The results detailed in this report focus on two of the eight mutants reported in previous work.[19] The Phe and Trp mutants behave in a similar fashion to native protein, while the Arg, Cys, Gln, and Ser mutants proved to be too unstable for the studies described herein. However, the Leu and His mutants were of moderate stability and were amenable to the approach detailed below. These studies provide insight on the functional (and structural) role of specific residues with regard to the regulation of solvent accessibility, and illustrate the use of multinuclear NMR methods (in one- and two-dimensions) to map out the solvent accessibility of HiPIP as a function of oxidation state in native and mutant proteins. These are issues of general relevance for structure/function studies of metalloredox proteins.

$^1H-^{15}N$ HMQC To Probe Backbone Amide Proton Exchange. Since $^1H-^{15}N$ coupling is over one bond, the intensity of cross-peaks in a $^1H-^{15}N$ HMQC experiment does not depend on backbone conformation, per se. This contrasts with the intensity of cross-peaks (and the magnitude of coupling constants) in the fingerprint region of a homonuclear $^1H,^1H$-COSY experiment, which results from a three ($H-N-C^{\alpha}-H$), or higher (in the case of a TOCSY experiment) bond correlation that will vary with a change of backbone dihedral angles. Accordingly, the rate of change of the intensities of $^1H-^{15}N$ cross-peaks for a lyophilized sample dissolved in D_2O provides a direct measure of the accessibility of solvent to the backbone amides, and permits an evaluation of the $^1H/^2H$ exchange rate. The selected mutants (Tyr19Leu and Tyr19His) for this study are of intermediate stability and display appropriate rates of exchange. Data could not be obtained for the oxidized forms as a result of the hydrolytic instability and very short half-life of this state.[19]

The exchange of ^1H by ^2H for the backbone amide protons was monitored by the decay and disappearance of the $^1H-^{15}N$ cross-peaks in HMQC spectra. These were recorded at a regular series of time intervals after dissolving the lyophilized sample

(22) Agarwal, A.; Tan, J.; Eren, M.; Tevelev, A.; Lui, S. M.; Cowan, J. A. *Biochem. Biophys. Res. Commun.* **1993**, *197*, 1357−1362.
(23) Li, D.; Cottrell, C. E.; Cowan, J. A. *J. Protein Chem.* **1995**, *4*, 115.
(24) Li, D.; Soriano, A.; Cowan, J. A. *Inorg. Chem.*, in press.
(25) Bax, A.; Griffery, R. R.; Hawkins, B. L. *J. Magn. Reson.* **1983**, *55*, 301.
(26) Bax, A.; Ikura, M.; Kay, L. E.; Torchia, D. E. Tshudin, R. *J. Magn. Reson.* **1986**, *86*, 304.

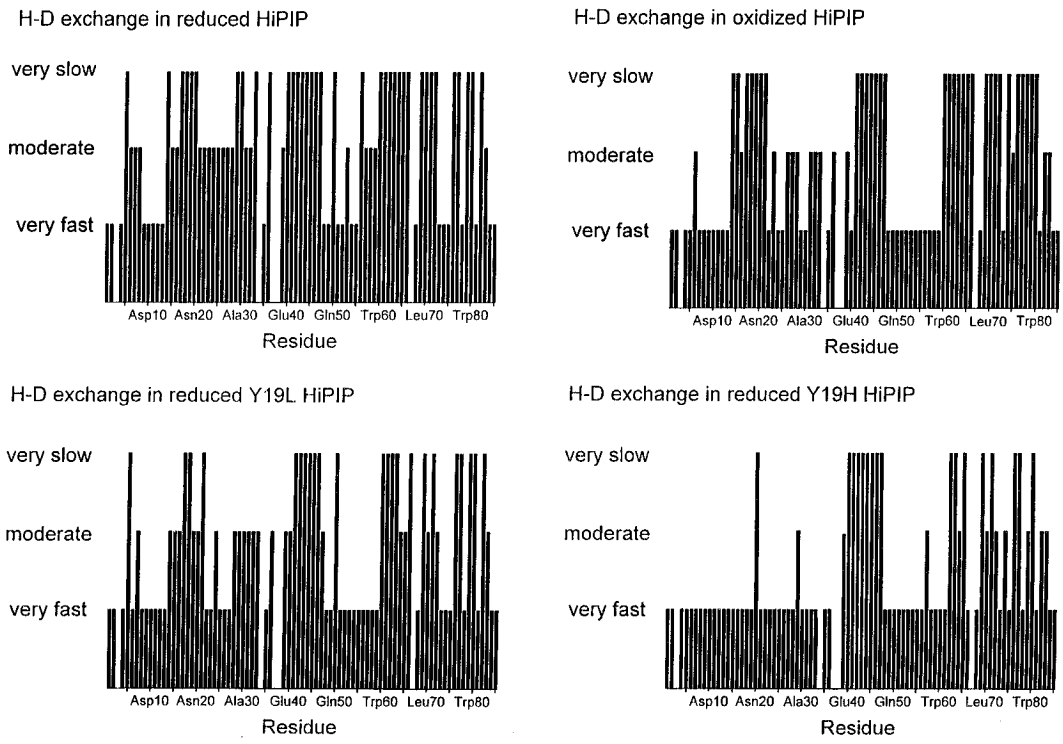

Figure 2. Scale bar presentation of $^1H/^2H$ exchange rate for backbone amide protons in the native and mutant proteins. Data could not be obtained for the oxidized mutant proteins as a result of the hydrolytic instability of this state.[19] The missing bars correspond to the proline residues at positions 3, 34, 37, 38, and 67, which lack an amide proton.

in D_2O. Each spectrum required a time of 8−12 min for completion prior to the next acquisition. Figure 1 shows examples of a series of spectra collected for reduced native HiPIP, and for the Tyr19Leu mutant. The exchange rates of assigned backbone amide protons[11,23] have been classified as slow, moderate, or fast (Figure 2), and designated by color coding in the backbone traces shown in Figure 3. Those residues where the $^1H-^{15}N$ cross-peaks remain visible at the end of a 7 to 8 h experiment lie in regions defined as showing *very slow exchange* (red in Figure 3). Residues that show cross-peaks that can be seen in the first spectrum, but not in the last one, exhibit *moderate exchange* rates (yellow in Figure 3). The remaining residues, the cross-peaks of which do not show in the spectrum immediately after redissolving in D_2O, belong to the *very fast exchange* region (blue in Figure 3).

The results summarized in Figures 2 and 3 lead to several conclusions. First, there is no significant difference in the $^1H/^2H$ exchange regimes observed for the reduced relative to the oxidized form of recombinant native HiPIP. Second, many residues lie in the very slow exchange regime for native HiPIP (and show cross-peaks in the $^1H-^{15}N$ HMQC spectra at the end of the experiment) in contrast to the smaller number of peaks observed for the mutant proteins. Third, in all samples, the four cluster-binding cysteines and their neighboring residues lie in the very slow exchange region. Finally, the backbone amide of Tyr19 and neighboring residues are found to lie in the slow exchange regime in the native protein, but switch to the moderate or very fast exchange regimes in the Tyr19Leu and Tyr19His mutant HiPIP's.

^{19}F NMR Parameters as a Probe of Solvent Accessibility. Fluorine-19 NMR resonances exhibit a strong environmental dependence, and provide a useful complement to the $^1H/^2H$ exchange experiments just described earlier.[27,28] It has been observed that both the chemical shift and T_1 relaxation time are sensitive to interaction with the solvent. When ^{19}F is solvent exposed the T_1 relaxation times become longer[27,29] and the ^{19}F resonance frequency shows an isotopic shift when the aqueous solvent is changed from H_2O to D_2O.[30,31] This solvent shift

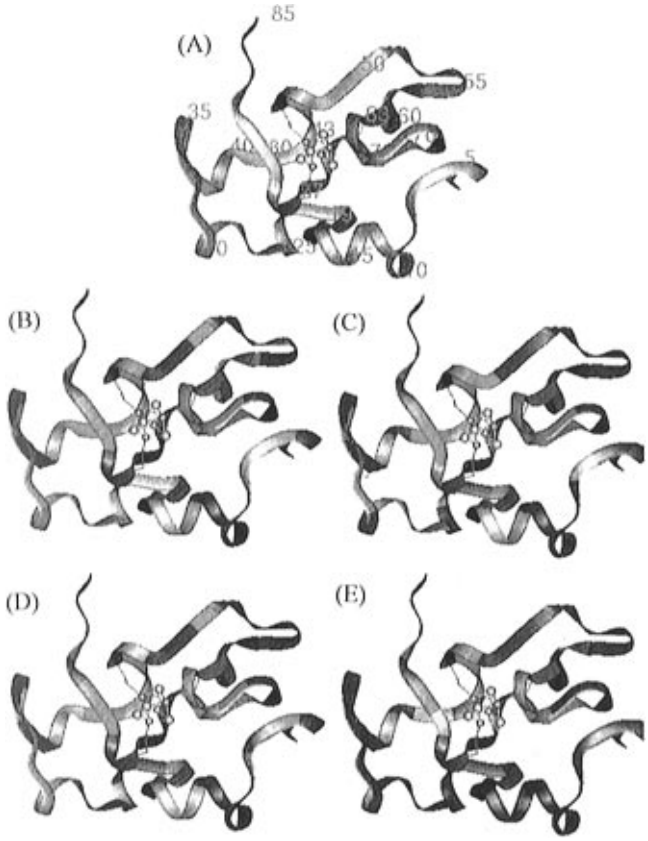

Figure 3. Color-coded presentation of $^1H/^2H$ exchange rate for amide protons is given for reduced (B) and oxidized (C) recombinant native and the reduced Tyr19Leu (D) and Tyr19His (E) mutants. The exchange regimes are color-coded: red = very slow, yellow = moderate, and blue = very fast. These exchange rates are defined in the text. The backbone numbering scheme is illustrated in part A.

(27) Gerig, J. T. *Methods Enzymol.* **1986**, *177*, 3−23.
(28) Gerig, J. T. *Prog. Nucl. Magn. Reson.* **1994**, *26*, 293.

Table 1. ^{19}F NMR Solvent Isotopic Shifts and Relaxation Times of the 3-F−Phe Derivatives of Tyr19Leu andTyr19His Mutant HiPIP's

	reduced			oxidized		
Tyr19Leu param	Phe48	Phe(-1)[a]	Phe66	Phe48	Phe(−1)	Phe66
δ (ppm), in H_2O	−38.41	−38.08	−37.59, −37.87	−37.13	−37.88	−40.37
δ (ppm), in D_2O	-38.56	−38.24	−37.58, −37.90	−37.25	−38.16	−40.37
$\Delta\delta$ (ppm), mutant[b]	0.15	0.16	0.01, 0.03	0.12	0.28	0.0
$\Delta\delta$ (ppm), native[b,c]	0.06	0.12	0.01	0.12	0.09	0.07
T_1 (s), mutant	0.23	0.65	0.12	0.13	0.69	0.02
T_1 (s), native[c]	0.13	0.67	0.05	0.21	0.65	0.03

	reduced		
Tyr19His param	Phe48	Phe(−1)[a]	Phe66
δ (ppm), in H_2O	−38.45	−38.13	−37.66, −37.89
δ (ppm), in D_2O	−38.57	−38.24	−37.50, −37.98
$\Delta\delta$ (ppm), mutant[b]	0.12	0.11	0.16, 0.09
$\Delta\delta$ (ppm), native[b,c]	0.06	0.12	0.01
T_1 (sec), mutant	0.17	0.56	0.053
T_1 (sec), native[c]	0.13	0.67	0.045

[a] Phe(−1) is an additional Phe residue resulting from the gene construct.[22] It provides a useful control as a solvent exposed surface residue. [b] Typically $\Delta\delta$ must exceed 0.1 ppm to indicate a bona fide solvent effect. This represents a frequency shift of 23.5 Hz, which is readily detectable. [c] From ref 24 for comparison.

should be greater than 0.1 ppm to be of significance. In general T_1 measurements are less reliable than the isotopic shift as a probe of solvent accessibility for proteins that contain paramagnetic cofactors, since the paramagnetic relaxation mechanism may also reduce the relaxation time.

Both T_1 values and isotopic shifts in ^{19}F resonances for 3-F−Phe-labeled Tyr19Leu and Tyr19His mutants were measured and compared with data collected for the 3-F−Phe-labeled native protein. The F-Phe group provides a nonperturbative probe of local structure and dynamics.[24] Illustrative ^{19}F NMR spectra are shown in Figure 4, and specific assignments of ^{19}F resonances to fluorine-labeled Phe residues have been made previously on the basis of results from mutational analysis of Phe66 and Phe48.[24] The resonance ascribed to Phe(−1) derives from an additional Phe residue that was added during construction of the synthetic gene.[22] For Phe48, both the longer T_1 and larger isotopic shifts for the ^{19}F resonances indicate that Phe48 is more solvent exposed in the mutant proteins than in native HiPIP. For Phe66, there is no significant isotopic effect for either the native protein or the Tyr19Leu mutant in either oxidation state. Table 1 shows a large isotopic shift for the Tyr19His mutant in the reduced state, which is consistent with an increase in solvent exposure and the known relative stabilities of the His and Leu mutants.[19] Data could not be obtained for the oxidized form as a result of the very short half-life of this state.

For both Tyr19Leu and Tyr19His mutants two peaks are observed for the ^{19}F NMR signal from Phe66 in the reduced state (Table 1 and Figure 4), but only one signal was seen in the oxidized state. This data demonstrates that the rotation of Phe66 becomes slower in the reduced mutants than is observed for the reduced native HiPIP. This mirrors the situation observed for 3-F−Tyr19-labeled native HiPIP, previously reported from our laboratory.[18] In that case we deduced that the close interaction between Tyr19 and the reduced cluster in native HiPIP resulted in a slow rate of rotation around the C^{β}−C^{γ} bond. Interestingly, Phe66 also lies close to the cluster[24] and is presumably experiencing hindered rotation in the reduced mutants, although this is not observed for either oxidation state of the native protein. Since Tyr19 and Phe66 are not close to each other in space,[1] the change of rotation may result from a minor conformational variation induced by the mutation. One possibility may be that Phe66 moves closer to the cluster.

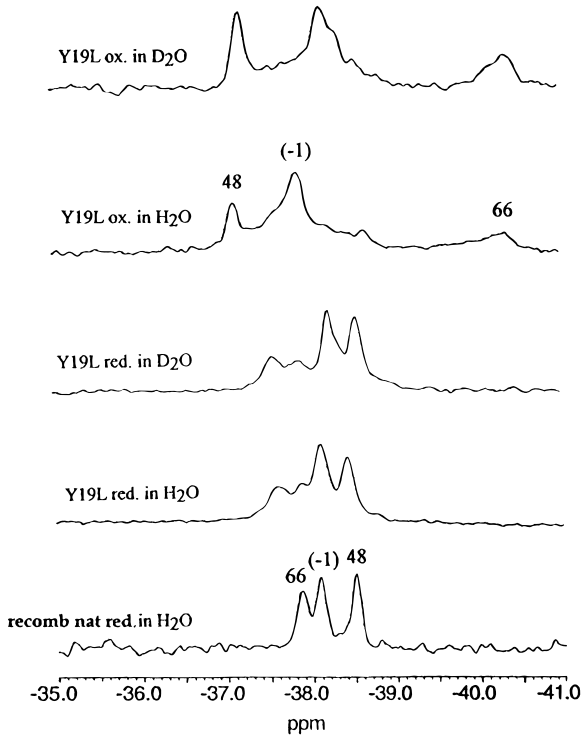

Figure 4. ^{19}F NMR spectra of 3-F−Phe-labeled Tyr19Leu and Tyr19His mutants recorded in H_2O and D_2O, respectively. The ^{19}F NMR of reduced 3-F−Phe labeled native HiPIP is included to highlight the splitting of one resonance in the reduced mutant forms, as described in the text. Assignments are indicated on representative spectra.

Discussion

In this paper we have focused on the Leu and His mutants of Tyr19.[19] Figures 2 and 3 show the solvent accessibility of the peptide backbone as determined from the rate of exchange of backbone amide protons by ^{1}H−^{15}N HMQC experiments. The increase of ^{1}H/^{2}H exchange from native to the mutants indicates that the conformation of mutants is more "open" than that of native HiPIP. Tyrosine 19 lies in a slow exchange region in native HiPIP, but this domain shows fast exchange for the mutant proteins. All four cysteine residues and their immediate neighbors lie in an hydrophobic environment. Another sequence

(29) Drake, S. K.; Bourret, R. B.; Luck, L. A.; Simon, M. I.; Falke, J. J. *J. Biol. Chem.* **1993**, *268*, 13081.
(30) Gerig, J. T. *Bio. Magn. Reson.* **1978**, *1*, 139.
(31) Hansen, P. E.; Dettman, H. D.; Sykes, B. D. *J. Magn. Reson.* **1985**, *62*,487.

of interest lies in the domain from residues 22 to 38. For these residues, $^1H/^2H$ exchange lies in the slow to moderate range in native HiPIP, but moves to very fast exchange for the mutants. These results suggest that these mutations change the solvent accessibility not only around Tyr19 but also around other residues in the cluster-binding pocket.

The change in solvent accessibility suggested by the amide proton exchange data is further supported by the isotope effect on ^{19}F chemical shifts for 3-F−Phe-labeled native and mutant HiPIP's (Table 1). The largest effect is observed for Phe66, which lies in the solvent exposed domain revealed in the Leu and His mutants (Figure 3). Also, the splitting observed for the ^{19}F resonance of 3-F−Phe66 in the reduced Tyr19Leu and Tyr19His mutants is consistent with a closer interaction with the [Fe_4S_4] cluster, which inhibits free rotation around the $C^{\beta}-C^{\gamma}$ bond. As for Tyr19, residue Phe66 lies in close proximity to the [Fe_4S_4] cluster. In contrast to Tyr19, however, which appears to form an intimate complex with the reduced cluster in native protein,[8] Phe66 appears to complex only after minor conformational changes induced by the mutation of Tyr19.

Earlier crystallographic studies demonstrated that the hydroxyl of Tyr19 in native HiPIP forms a hydrogen bond contact to the side chain of Asn72 and donates a hydrogen bond to a water molecule, while the aromatic side chain lies in close proximity to an inorganic sulfur in the reduced $[Fe_4S_4]^{2+}$ cluster.[8] The phenolic side chain effectively stretches across the entrance to the cluster binding pocket, forming a portal that excludes solvent water. For *C. vinosum* HiPIP, hydrogen bonding between Tyr19 and Asn 72 does not appear to be required to hold the side chain in place, since the Tyr19Phe mutant, which lacks the hydroxyl shows considerable stability relative to the native protein.[19] However, neither small nor polar residues are capable of preventing solvation of the cluster-binding pocket.

In conclusion, both the $^1H-^2H$ exchange and ^{19}F NMR experiments described here provide direct evidence for an increase in solvent accessibility following mutation of Tyr19 to small or polar side chains and support the functional model recently proposed for this residue.[19] Given the importance of determining solvent accessibility for the understanding of substrate binding chemistry in enzymes, and the modulation of the redox properties of prosthetic centers in metalloproteins and enzymes, the strategies illustrated herein should be of general interest and value.

Acknowledgment. Supported by the National Science Foundation (Grant CHE-8921468).

IC951160S